MASW Analysis of Bedrock Velocities (Vs and Vp)

Choon Park, Park Seismic LLC, Shelton, Connecticut, USA*

Summary

The dispersion image from an MASW field record unambiguously shows the high-frequency side asymptotic trend of dispersion curve that corresponds to surface wave velocity of soil. The low-frequency side asymptotic trend for bedrock, however, is rarely measured because it would require an impractically long receiver array to record such long wavelengths of surface waves (e.g., 50 times longer than bedrock depth). Bedrock velocities, however, can be depicted in dispersion images from the energy patterns created from refracted body waves, rather than surface waves, because refracted waves also travel horizontally along the surface. Both S and P waves are always generated regardless of the impact orientation of seismic source on the surface. The refraction would create a non-dispersive energy pattern that occurs at much higher frequency and phase velocity ranges (e.g., 50-300 Hz with 3000-15000 ft/sec) than those for surface waves (e.g., 5-50 Hz with 0-3000 ft/sec). This body-wave phenomenon appearing in dispersion images is described by using both a synthetic and two field records. A simple process is also described that estimates both S (Vs) and P (Vp) wave velocities of bedrock by summing amplitudes of dispersion image along the frequency axis.

Introduction

The multichannel analysis of surface waves (MASW) method (Park et al., 1999) is commonly used to characterize soil and bedrock in stiffness and depth to bedrock (Miller et al., 1999). First, using a 2D wavefield transformation method, a raw multichannel seismic record is transformed into a so-called dispersion image (Park et al., 1998; McMechan and Yedlin, 1981). This transformation collects all seismic wavefields travelling horizontally and then disposes the collected energy at the corresponding point in the frequency-phase velocity space from which a dispersion curve is extracted and inverted to generate a Vs profile (Xia et al., 1999). For an accurate inversion process, it is important for a measured dispersion curve to include phase velocities corresponding to both soil and bedrock. The asymptotic soil phase velocity is usually well resolved during most MASW analyses. On the other hand, the asymptotic bedrock phase velocity is almost always not measured because the corresponding wavelength is tens of times longer than the bedrock depth. Measurement of such a long wavelength would require deployment of an impractically long receiver array (e.g., 50 times longer than depth to bedrock).

Body waves (P and S) can always generate bedrock refractions, on the other hand. Both P and S waves are always generated simultaneously, regardless of the impact orientation at the source point (Pugin et al., 2010). In consequence, on a typical MASW field record, the P-wave refraction would appear as a linear event, commonly called "first arrivals", and then the S-wave refraction will follow at a later time where surface waves and other body waves also appear. Both P- and S-wave refractions from the bedrock can be repeated several times due to multiple reflections within a soil layer that may also include mode-converted reflections.

Waves refracted from bedrock travel horizontally, as do surface waves. Although surface waves are usually dispersive, refracted waves are not dispersive and all frequency components travel at the same phase velocity. Surface waves usually take relatively low frequencies (e.g., 5-30 Hz), while refractions take much higher frequencies (e.g., 50-250 Hz). On a dispersion image obtained from an MASW field record these refracted waves would appear as a non-dispersive energy pattern (i.e., a straight line in parallel to the frequency axis) that occurs not at the usual frequency range for surface waves (e.g., 5-30 Hz), but at higher frequencies (e.g., 50-300 Hz).

MASW Analysis of Soil and Bedrock

The MASW evaluation of soil and bedrock includes, in general, the estimation of soil S-wave velocity (Vs-so), bedrock S-wave velocity (Vs-bd), and bedrock depth (Z-bd). An accurate evaluation of bedrock depth (Z-bd) is highly related to an accurate measurement of the deflecting point where the asymptotic soil phase velocity starts to deviate toward higher phase velocities. To illustrate the relative effectiveness of each of the three parameters, a synthetic seismic record generated by using the reflectivity modeling scheme (Fuchs and Muller, 1971) based on a layered-earth model is displayed in Figure 1a. A vertical source was assumed and the displayed seismic record represents the vertical (V) component of seismic waves. The dispersion image processed from this record is displayed in Figure 2a, with the theoretical fundamental-mode (M0) dispersion curve displayed in Figure 2b. Both asymptotic soil phase velocity and the deflection point of the curve are clearly imaged, indicating both Vs-so and Z-bd can be accurately estimated from MASW analysis. The lowest frequency part of the image stops at about 4 Hz, however, where phase velocity is only about 20% of the bedrock phase velocity. This indicates that the bedrock velocity (Vs-bd) will be severely underestimated from the MASW analysis.

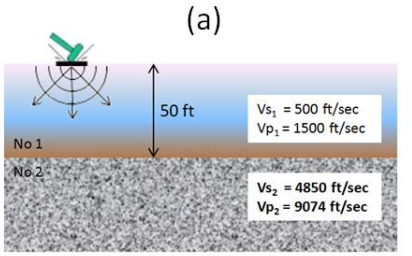

No	Depth (ft)	density (g/cc)	POS	Qs	Qp
1	50	1.75	0.438	6	7
2	Half Space	2.0	0.300	30	35

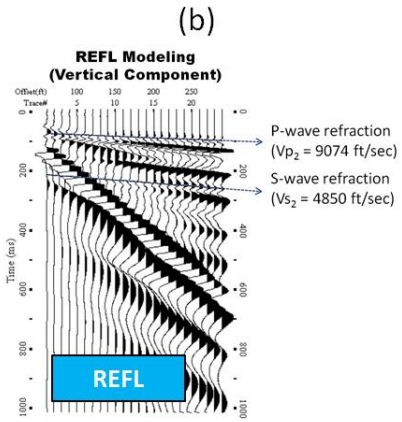

Acquisition channel:	24
Receiver spacing (dx):	10 ft
Source offset (X1):	30 ft
Source spectrum (Hz):	1-5-400-450

Figure 1: (a) A layered-earth model used for reflectivity modeling to generate the synthetic MASW record in (b).

Bedrock Refractions Observed in Dispersion Image

Figure 3a shows a dispersion image processed from the synthetic record displayed in Figure 1b, but obtained using a much broader-range process in frequency and phase velocity. This image shows two apparently non-dispersive energy patterns appearing at phase velocities close to S and P velocities, respectively, of bedrock. Their dominating frequencies are in the approximate range from 25-100 Hz and 100-200 Hz, respectively, being much higher than that for surface waves (e.g., 4-25 Hz). The synthetic seismic record in Figure 1b clearly shows the P-wave refraction as first arrivals occurring with correct phase velocity and with apparent frequencies close to those frequencies observed in the dispersion image. However, S-wave refraction is not so obvious on the seismic record because it would appear at later times where other types of arrivals (e.g., reflections and surface waves) also exist. Analytical arrival times corresponding to the S-wave refraction, however, are indicated by a straight line on the record in Figure 1b. A seismic arrival pattern is identified near this line that has apparent frequencies close to those of the other energy pattern observed in the dispersion image, confirming the other energy pattern originates from the S-wave refraction.

Figure 3b shows theoretical dispersion curves generated from the elastic-earth model presented in Figure 1a for the fundamental-mode (M0) and fifty higher modes (M1-M50). It shows all dispersion curves get close to each other at those phase velocities corresponding to all subsurface seismic velocities. The closeness at soil S velocity (Vs_1) seems to be most prominent, and then those at soil Vp (Vp_1), bedrock Vs (Vs_1), and bedrock Vp (Vp_2) become prominent to a lesser extent. The dispersion image in Figure 3a confirms three velocities out of four—Vs_1, Vs_2, and Vp_2. The soil P-wave velocity (Vp_1) would be imaged if horizontal (radial) component of the modeled seismic record is used for this dispersion image because direct P-wave arrivals are basically radial components.

Dispersion images processed from actual field records acquired at two wind-turbine sites in the Northeast US are displayed in Figure 4. They were acquired using a 24-channel system with a 10-ft receiver spacing and a 30-ft source offset. A 10-lb sledge hammer was used as source. The surface-wave dispersion images (Figures 4a and 4b) clearly show the asymptotic soil phase velocities of the two

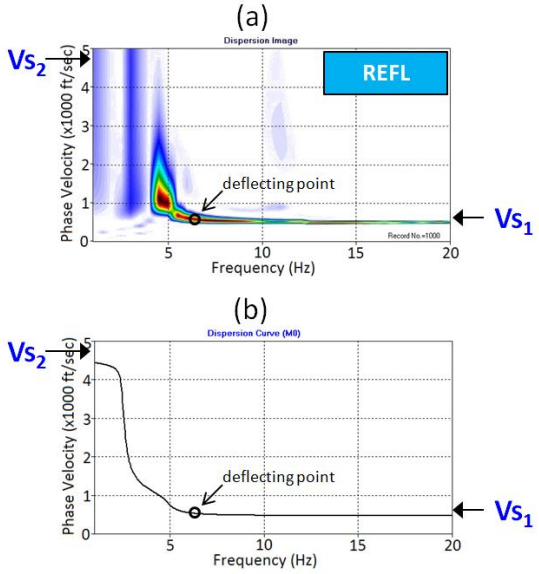

Figure 2: (a) Dispersion image processed from the synthetic record in Figure 1(b), and (b) a theoretical fundamental-mode (M0) dispersion curve for the model in Figure 1(a).

sites. However, on the low-frequency side both images virtually terminate at about 4 Hz with a phase velocity only approaching 1000 ft/sec, which is significantly lower than standard rock velocities (e.g., ≥ 2500 ft/sec). This indicates that bedrock velocity (Vs) cannot be accurately resolved through normal MASW analysis. On the other hand, the two broad-range dispersion images (Figures 4b and 4d) show two strong energy patterns at higher frequencies (e.g., ≥ 50 Hz). The lower-frequency energy pattern has the lower phase velocity, indicating that it originates from the S-wave refraction. The other energy pattern takes higher frequencies and phase velocities, indicating that it originates from the P-wave refraction. The energy patterns observed at site 13, however, are extremely narrow-banded in nature. The phase velocities corresponding to the S- and P-wave refractions, respectively, occur almost at the same two velocities for the two sites, indicating that the two sites share a common bedrock.

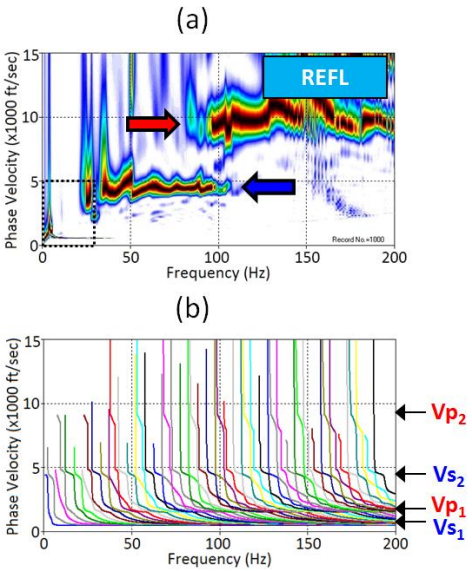

Figure 3: (a) Dispersion image processed from the synthetic record in Figure 1(b) using a broad range in frequency and phase velocity. The portion highlighted at lower left indicates the range used for Figure 2(a). (b) Theoretical dispersion curves for the model in Figure 1(a) in the fundamental-mode (M0) and fifty higher modes (M1-M50).

Frequency Summation of Dispersion Image

The energy pattern of a refraction appearing in a dispersion image is always distorted due to interference of other energy patterns created from body-wave events (e.g., reflected and scattered waves of seismic and acoustic origins) as well as from computational artifacts (e.g., boundary effects and spatial aliasing effects). To improve the ability to estimate this phase velocity, all amplitudes in a dispersion image can be stacked along the frequency axis. This process constructively adds all those amplitudes aligned along a straight line and results in a peak in the summed amplitude curve occurring at the most probable phase velocity the observed energy pattern may represent.

This frequency-summation process (FRQ-Sum) is graphically illustrated in Figure 5 by applying the process to dispersion images of the synthetic record and two field seismic records previously described. Comparing values of the two peaks in the summed curve from the synthetic record (4540 ft/sec and 9470 ft/sec, respectively) to true values (Vs_2=4850 ft/sec and Vp_2=9074 ft/sec), they are accurate within 94% and 95%, respectively. Vs and Vp peaks observed in the summed curves from the two field records indicate the possible bedrock velocities can be Vs=4460 ft/sec and Vp=9420 ft/sec at site 12, and Vs=4340 ft/sec and Vp=9620 ft/sec at site 13. Then, Poisson's ratios are calculated as 0.356 (site 12) and 0.372 (site 13), respectively. The differences between the two Vs values and the two Vp values from the two sites are less than 3%, while the difference in Poisson's ratio is about 4%. Definition of the Vp peak at site 13 is extremely low because of the narrow-banded nature of the corresponding energy pattern.

Discussions

The refraction energy patterns may or may not appear in the dispersion image processed from an MASW field record; that is, both P- and S-wave refractions may be there, or only one of them, or possibly neither of them can be identified. There are several factors controlling this: (1) receiver array length (L), (2) attenuation property of soil (Qs_1 and Qp_1), (3) velocity contrast between soil and bedrock, and (4) seismic source characteristics in the order of relative significance. Impact of these factors will be further elaborated in the future publications.

Receivers have to be placed at a distance further than the critical distance for refraction (Xc) to occur. Xc is determined from the velocities of soil and bedrock (V1 and V2) and bedrock depth (Z-bd); $X_c = 2Z_{bd}/\sqrt{(V_2/V_1)^2 - 1}$ (Sheriff and Geldart, 1982). The common guideline for MASW acquisition geometry suggests that array length (L) and source offset (X1) should be L ≥ 2Z-bd with X1 ≥ (1/2)Z-bd. This condition puts the array well beyond Xc in most cases for both S (Xc-s) and P (Xc-p) refractions. For example, the critical distances for the model in Figure 1a

are calculated as Xc-s ≈ 10 ft and Xc-p ≈ 17 ft, while the optimum X1 for MASW would be 50 ft. This means most MASW field records must contain refractions from bedrock, which might have not been detected simply because the normal analysis range was focused only on surface waves (e.g., 1-50 Hz with 0-5000 ft/sec).

The longer array length enhances resolution of energy patterns in the dispersion image (Park et al., 2001). In addition, more spatial data points provided from more acquisition channels will always increase the total energy of recorded refractions. In this sense, an MASW acquisition with a long array (e.g., L ≥ 3Z-bd) deployed with many receivers (e.g., 48) can increase the overall resolution of the analysis.

Conclusions

The conclusions of this study are as follows;

- MASW field records can be processed to get information about bedrock velocities (Vs and Vp), not from the surface-wave phenomenon but from the body-wave (refraction) phenomenon.
- For this, the range in frequency and phase velocity has to be significantly expanded during the construction of the dispersion image. For example, an optimum range would be 1-300 Hz in frequency, and 0-15000 ft/sec in phase velocity.
- The frequency summation (FRQ-Sum) method that sums amplitudes in dispersion images along the frequency axis can be a simple but highly effective tool to estimate S- and P-wave velocities (Vs and Vp) of bedrock.
- A longer receiver array with more channels than commonly recommended for an MASW survey will increase the overall resolution of the analysis.

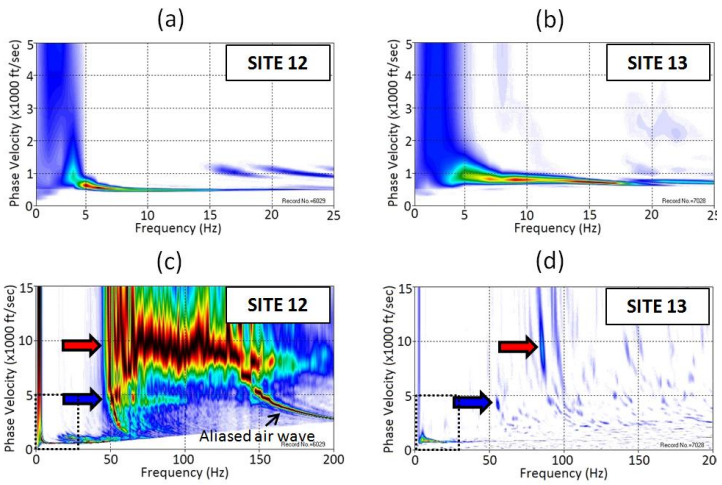

Figure 4: Dispersion images processed from field MASW records obtained from two wind-turbine sites, (a) site 12 and (b) site 13. Broad-range dispersion images for the two records are displayed in (c) and (d), respectively. The portion highlighted at lower left in (c) and (d) indicate the range used in (a) and (b).

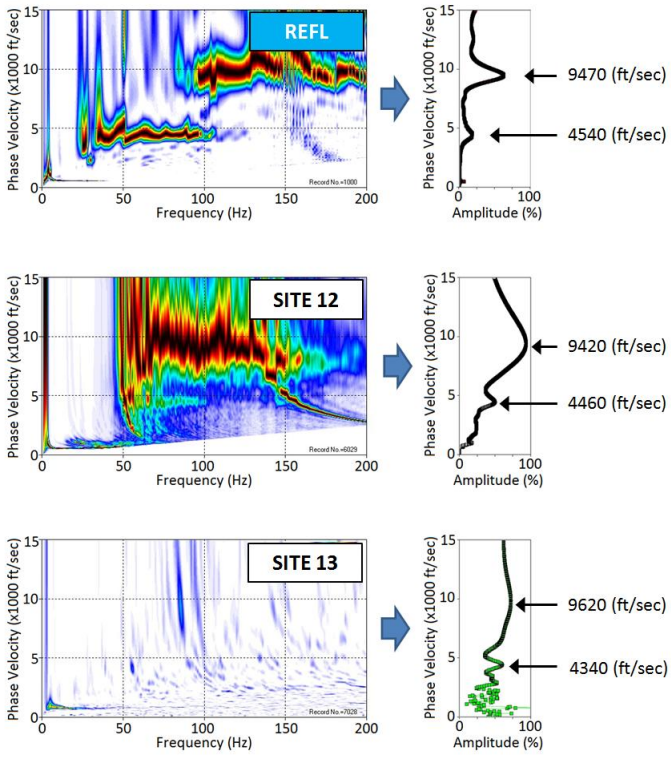

Figure 5: Illustration of the frequency-summation (FRQ-Sum) method applied to the synthetic (REFL) and the MASW records from sites 12 and 13.

RFERENCES (Submitted Separately)

Fuchs, K., and Muller, G., 1971, Computation of synthetic seismograms with the reflectivity method and comparison with observation: Geophys. J. Roy. Astr. Soc., **23**, 417-433.

McMechan, G., and Yedlin, M.J., 1981, Analysis of dispersive waves by wave field transformation, Geophysics, v. 46, n. 6, p. 869-874.

Miller, R.D., Xia, J., Park, C.B., and Ivanov, J.M., 1999, Multichannel analysis of surface waves to map bedrock, Kansas Geological Survey, The Leading Edge, December, p. 1392-1396.

Park, C.B., Miller, R.D., and Xia, J., 2001, Offset and resolution of dispersion curve in multichannel analysis of surface waves (MASW): Proceedings of the SAGEEP 2001, Denver, Colorado, SSM4.

Park, C.B., Miller, R.D., and Xia, J., 1999, Multichannel analysis of surface waves: Geophysics, v. 64, n. 3, pp. 800-808.

Park, C.B., Miller, R.D., and Xia, J., 1998, Imaging dispersion curves of surface waves on multi-channel record: 68th Ann. Internat. Mtg. Soc. Expl. Geophys., Expanded Abstracts, p. 1377-1380.

Pugin, A.J.M., Pullan, S.E., and Hunter, J.A., 2010, Update on recent observations in multi-component seismic reflection profiling: Symposium on the Application of Geophysics to Engineering and Environmental Problems (SAGEEP 2010), Keystone, Colorado, April 11-15.

Sheriff, R.E., and Geldart, L.P., 19882, Exploration seismology, vol 1: history, theory, and data acquisition: Cambridge University Press.

Xia, J., Miller, R.D., and Park, C.B., 1999, Estimation of near-surface shear-wave velocity by inversion of Rayleigh waves: Geophysics, v. 64, n. 3, p. 691-700.